https://doi.org/10.1007/s41230-018-7104-8

Ignition-proof performance and mechanism of AZ91D-3Nd-*x*Dy magnesium alloys at high temperatures

Yong-yan Li, Wei-min Zhao, Jian Ding, and *Hai-tao Xue

School of Materials Science & Engineering, Hebei University of Technology, Tianjin 300132, China

Abstract: This study focused on the synergistic effect of alloying elements neodymium (Nd) and dysprosium (Dy) on the ignition-proof performance of AZ91D alloy. The ignition-proof mechanism of AZ91D-3Nd-*x*Dy (x = 0.5, 1.0, 1.5, 2.0 and 2.5wt.%) alloy was discussed in depth through ignition-proof testing and microstructure observation. The results showed that the AZ91D-3Nd-2Dy alloy exhibited the highest ignition-point of 893 K, increased by 69 K as compared to the AZ91D alloy. The ignition-proof mechanism of Nd and Dy additions lay in three aspects: (1) the formation of denser oxide film consisting of Dy_2O_3 and MgO improves the oxidation resistance of the alloy, (2) the great reduction of the low melting-point phase β-$Mg_{17}Al_{12}$, which leads to the decrease in the oxygen diffusion channels, and (3) the newly formed high melting-point phases (Al_2Nd and Al_2Dy), which block the oxygen diffusion channels and prevent the chemical reaction of Mg and oxygen.

Key words: AZ91D; Nd; Dy; ignition-proof; high temperature

CLC numbers: TG146.22 **Document code:** A **Article ID:** 1672-6421(2018)02-097-06

Mg alloys are widely used in automobile, electronics, and aerospace fields due to their good properties such as high specific strength, high stiffness, good shock-proof and electromagnetic shielding performance, etc [1,2]. The application of Mg alloys, however, is still relatively limited because of their easily induced oxidation and ignition at high temperatures, which brings many difficulties during the melting and processing of Mg alloys. To improve the ignition-proof performance of Mg alloys, researchers have developed many methods, among which, flux and inert gases coverage are effective ways to prevent Mg alloys from being oxidized and ignited. Nevertheless, there are still some disadvantages such as induced impurities, environmental pollution, device complexity and so on [3-8].

In the 1950s, a simple method was developed to enhance the ignition-proof performance of Mg alloys by adding alloying elements [5-8]. During the process of melting, the highly protective oxide film can be spontaneously formed on the surface of Mg alloys due to the enrichment of alloying elements on the surface, which could prevent further oxidation or even burning of Mg alloys. Based on this theory, many studies have been reported about the influence of additional elements on the ignition point of Mg alloys [5-12]. The beryllium (Be) and RE additions effectively improved the ignition-proof performance of AZ91D alloy[5]. The Mg alloys could be melted without any flux and protective gas when the Be addition was up to 0.1wt.%. Lin P Y et al [9]. found that the addition of cerium (Ce) can increase the oxidation resistance of AZ91D and AM50 alloys. The ignition point reached 798 K for AZ91D alloy with 0.25wt.% Ce addition, and 808 K for AM50 alloy. As summarized in the previous research, it is commonly believed [5-6, 9-11] that the main reason for ignition-proofing is that the continuous and dense oxide film replaces the porous oxide film by adding alloying element during melting. It is well known that the diffusion rate of the atoms at liquid state is very high, which facilitates the forming of the protective oxide film rapidly at the molten alloy surface. However, as the diffusion rate of the atoms at solid state is much lower, the alloying element is unlikely to enrich on the surface and form the continuous and dense oxide film at solid state. Therefore, it is necessary to study the reason for the increase of ignition-point before the alloy is melted.

Some literature shows that adding Nd or Dy element can improve the ignition-point of Mg alloys [13]. However, there is no data about the combined effect of Nd and Dy on ignition-proof performance of AZ91D

***Hai-tao Xue**

Male, born in 1974, Ph. D., Associate Professor. Research interests: light metals and their weldability.

E-mail: xuehaitao@126.com

Received: 2017-07-25; Accepted: 2018-01-12

alloy. In this paper, the effect of Nd and Dy combined additions on ignition-proof performance of AZ91D alloy was investigated. The experimental results by our team show that in the AZ91D-Nd-Dy alloy system, the best ignition-proof performance can be obtained as Nd is 3.0wt.% and Dy is in the range of 0.5–2.5wt.%. So, the ignition performance and micrstructure of AZ91D-3Nd-*x*Dy (*x* = 0.5, 1.0, 1.5, 2.0 and 2.5wt.%) alloy were studied. Furthermore, the ignition-proof mechanism of the AZ91D-3Nd-2Dy alloy was discussed in depth.

1 Experimental procedures

1.1 Samples preparation

AZ91D master alloy was prepared by using commercial grades of Mg, Al, Zn and Mn with purity of 99.9wt.%. AZ91D-3Nd-*x*Dy (*x* = 0.5, 1.0, 1.5, 2.0 and 2.5wt.%) alloy was obtained by adding different amounts of Mg-30wt.%Nd and Mg-30wt.%Dy intermetallics to AZ91D master alloy. The raw materials were added into a crucible which was preheated to 773 K in an electric resistance furnace, then heated up to 1,023 K and held for 30 min. Furthermore, the melted alloy was stirred under the protection of CO_2+SF_6 to ensure the composition homogeneity. The molten alloy was then poured into a permanent mold to obtain an ingot which was cut to samples with Φ12×15 mm^2 size for ignition-point test and 10×10×10 mm^3 size for oxidation experiment. All samples were polished before the testing.

The chemical compositions of AZ91D master alloy and Mg-RE intermetallics are shown in Tables 1 and 2, respectively.

Table 1: Chemical compositions of AZ91D master alloy (wt.%)

Al	Zn	Mn	Mg
9.2	0.7	0.35	Bal.

Table 2: Chemical compositions of Mg-RE alloys (wt.%)

	Nd/Dy	Al	Cu	Fe	Ni	Mg
Mg-Nd	29.35	0.018	0.003	0.017	0.002	Bal.
Mg-Dy	29.03	0.017	0.003	0.015	0.002	Bal.

1.2 Ignition-point testing

The ignition-point testing device is shown in Fig. 1. The sample was placed in the well-type electric resistance furnace, then the furnace was heated at the rate of about 4 K·min^{-1}, and the temperature-time curve was examined by the ignition-point testing system at the same time. When the Mg alloy ignited, a lot of heat would be released and lead to the formation of an inflection point in the temperature-time curve, which was defined as the ignition-point of Mg alloys.

1.3 Microstructure characterization

After the ignition-point testing, the alloy with the highest ignition-point was selected to analyze the ignition-proof mechanism. Phase identification was performed by X-ray diffraction (XRD, JEOL Rigaku 2500/PC) to obtain detailed information of the existing phases in the samples. A field emission scanning electronic microscope (FSEM, FEI NanoSem 430) equipped with energy dispersive spectroscopy (EDS) was used to observe the characteristics of the oxide film and substrate, and to examine the elemental distribution of the oxide film and substrate.

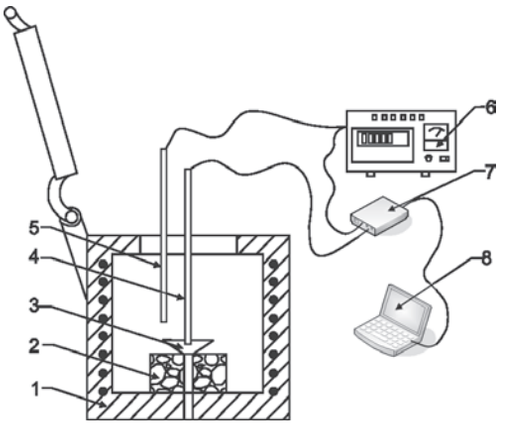

1. Electric resistance furnace; 2. Firebrick pad; 3. Crucible;
4, 5. Thermo-couple; 6. Temperature controller;
7. Data acquisition card; 8. Computer

Fig. 1: Schematic diagram of ignition-point testing system

2 Results and discussion

2.1 Ignition-proof performance

As shown in Fig. 2, the ignition-point of AZ91D alloy is 824 K. With the simultaneous addition of 0.5 to 2.5wt.% Dy and 3wt.% Nd to AZ91D alloy, the ignition-points are raised and the highest ignition-point of 893 K is reached with the composition of AZ91D-3Nd-2Dy. From the ignition-points testing curve, it can be seen that the simultaneous addition of Nd and Dy improves the ignition-point of AZ91D alloy, although all the samples ignite at solid state.

To further analyze the reason for the improvement of ignition-point with Nd and Dy additions, the structure characteristics and phase composition of AZ91D and AZ91D-3Nd-2Dy alloys at room temperature and high temperatures were comparatively analyzed.

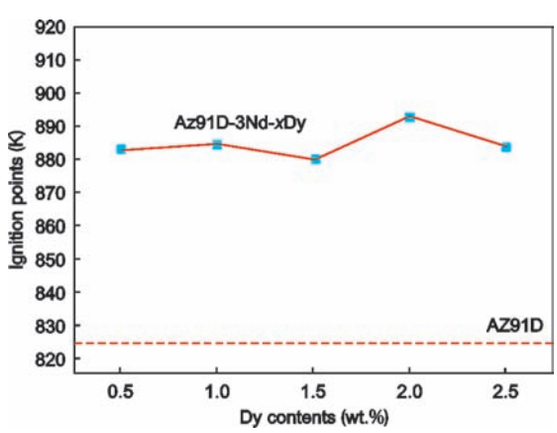

Fig. 2: Effect of Dy content on ignition-point of AZ91D-3Nd alloy

2.2 Microstructure and phase composition at room temperature

X-ray diffraction patterns of the as-cast AZ91D and AZ91D-3Nd-2Dy alloys are shown in Fig. 3. It can be identified that the as-cast AZ91D alloy consists of α-Mg and β-$Mg_{17}Al_{12}$ phases, while the as-cast AZ91D-3Nd-2Dy alloy consists of α-Mg and Al_2Nd along with minor β-$Mg_{17}Al_{12}$ phases.

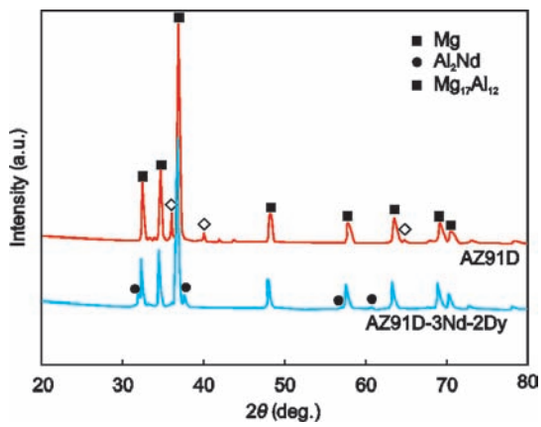

Fig. 3: XRD patterns of AZ91D and AZ91D-3Nd-2Dy alloys at room temperature

In order to further determine the distribution of the phases, SEM and EDS analyses were carried out. Figure 4 shows the microstructure morphologies of the as-cast AZ91D and AZ91D-3Nd-2Dy alloys at room temperature. It can be seen that there is a continuous network structure at the grain boundary for AZ91D alloy [Fig. 4(a)], while these networks become a dot structure for AZ91D-3Nd-2Dy alloy [Fig. 4(b)]. Combined with EDS analysis results (Table 3), it can be inferred that, for the AZ91D alloy, area A is the α-Mg substrate and area B located at the grain boundary is the β-$Mg_{17}Al_{12}$ phase companied with some α-Mg+β-$Mg_{17}Al_{12}$ eutectic phase. For the AZ91D-3Nd-2Dy alloy, the substrate (area C) is the same as that of AZ91D alloy, and the gray strip area (area D) located at the grain boundary is the α-Mg phase with minor α-Mg+β-$Mg_{17}Al_{12}$ eutectic phase, and the white dots (area E) at the grain boundary is the Al_2Nd phase with a little Al_2Dy phase. It should be noted that there was no appearance of the Al_2Dy phase in XRD patterns (Fig. 3), which is probably due to the low content of Dy and its high solubility in Mg substrate.

From Fig. 4(b), it is observed that the Al_2Nd and Al_2Dy phases disperse along the grain boundaries. Moreover, the formation of the new phases (Al_2Nd and Al_2Dy) leads to the consumption

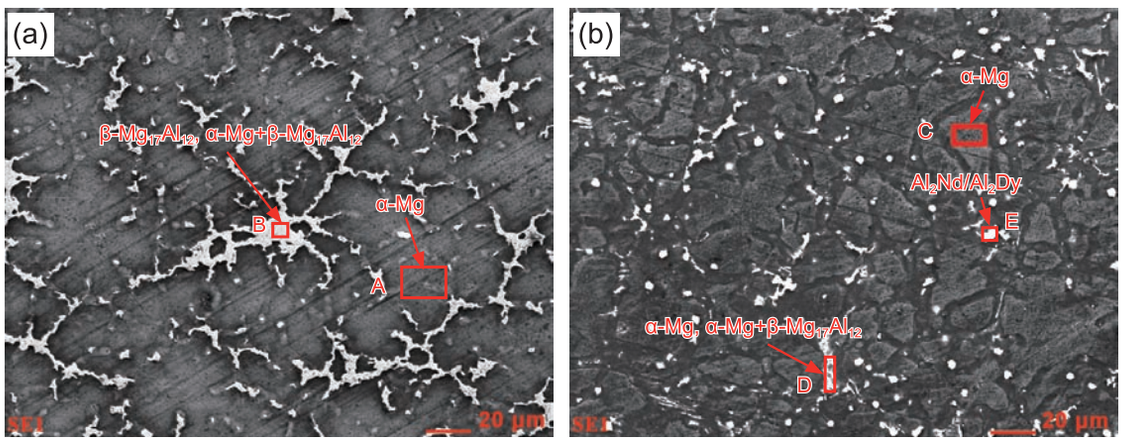

Fig. 4: Microstructures of as-cast alloys at room temperature: (a) AZ91D (b) AZ91D-3Nd-2Dy

Table 3: EDS analysis of locations in Fig. 4

Location	Elements (at.%)			
	Mg	Al	Nd	Dy
A	95.16	4.84	–	–
B	68.52	31.48	–	–
C	98.43	1.57	–	–
D	87.82	12.18	–	–
E	0	69.23	19.99	10.77

of Al, which results in the great decrease of β-$Mg_{17}Al_{12}$ and α-Mg+β-$Mg_{17}Al_{12}$ eutectic phases. Consequently, the distribution of β-$Mg_{17}Al_{12}$ and α-Mg+β-$Mg_{17}Al_{12}$ eutectic phases changes from continuous network along the grain boundaries for AZ91D alloy [Fig. 4(a)] to dispersion distribution for the AZ91D-3Nd-2Dy alloy [Fig. 4(b)].

2.3 High temperature oxidation experiment

For further clarify the ignition-proof mechanism of AZ91D-3Nd-2Dy alloy at high temperatures, the AZ91D and AZ91D-3Nd-2Dy alloys were heated to 773 K simultaneously, and held for 6 h to compare the difference of oxide film and substrate between two samples.

2.3.1 Surface morphology and phase composition of oxide film

The addition of Nd and Dy elements promotes the change of the AZ91D alloy in morphologies. Figure 5 shows the surface morphologies of the oxide film formed at the AZ91D and AZ91D-3Nd-2Dy samples after oxidation. It can be seen that there are many network cracks formed at the oxide film of the AZ91D alloy. In contrast, the oxide film of the AZ91D-3Nd-2Dy alloy is continuous and dense. It is known that AZ91D

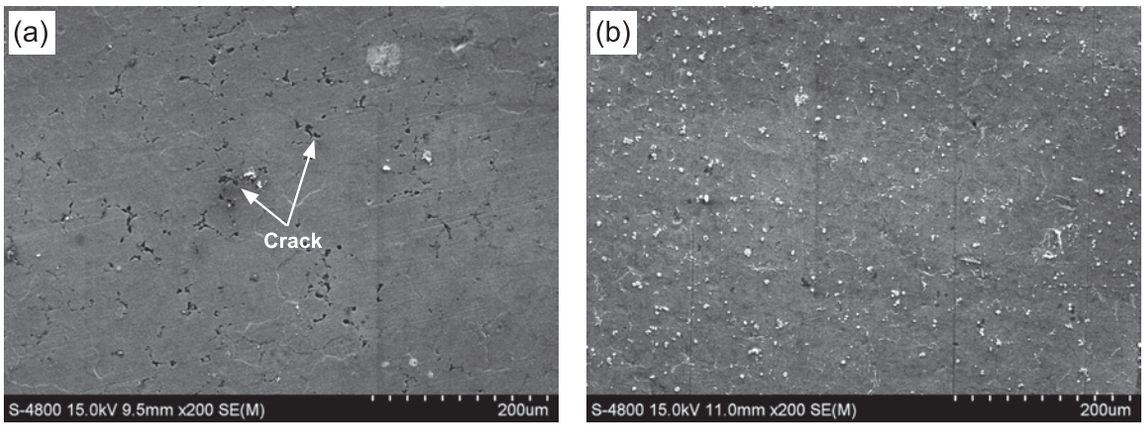

Fig. 5: Morphologies of surface oxide film at 773 K after holding for 6 h: (a) AZ91D; (b) AZ91D-3Nd-2Dy

alloy consists of α-Mg substrate and low melting point phase β-$Mg_{17}Al_{12}$ (the melting point is 710 K) located at the grain boundary at room temperature [Fig. (4a)]. The large amount of β-$Mg_{17}Al_{12}$ phase will preferentially melt at 773 K, which results in the network cracks formed at the grain boundary. The network cracks provide the passage for oxygen penetration, leading to the further oxidation and ignition of the alloy substrate. On the other hand, as described in section 2.2, for the AZ91D-3Nd-2Dy alloy, there is only minor β-$Mg_{17}Al_{12}$ phase dispersed along the grain boundaries due to the consumption of Al by Nd/Dy. Meanwhile, the Al_2Nd and Al_2Dy phases dispersed along the grain boundaries in the AZ91D-3Nd-2Dy alloy are both high melting point phases (the melting points are 1,733 K and 1,763 K, respectively [14-15]), and they are stable at 773 K. Therefore, there is no obvious crack formed in the AZ91D-3Nd-2Dy alloy at 773 K, which is the main reason for the increased ignition-point of AZ91D-3Nd-2Dy alloy.

Figure 6 shows the XRD patterns for the surface film of the AZ91D and AZ91D-3Nd-2Dy alloys formed at 773 K and held for 6 h. In Fig. 6, it can be found that MgO is the main oxide phase in the surface film of the AZ91D alloy. However, Dy_2O_3 is detected in the surface film of the AZ91D-3Nd-2Dy alloy beside MgO. In general, the dense oxide film formed in the surface of alloy can effectively prevent the diffusion of oxygen into the substrate. The tightness is always expressed by Pilling-Bedworth (P-B) ratio (ratio of the oxide volume to the consumed metal volume) [16]. When P-B ratio is <1.0, the oxide film is loose and has no protectiveness; when the P-B ratio >1.0, the oxide film is compact enough to protect the alloy from being oxidized. The P-B ratio of MgO/Mg is 0.81 [7], so the oxide film of AZ91D alloy composed of MgO exhibits poor protectiveness. For the AZ91D-3Nd-2Dy alloy, the oxide film is composed of MgO and Dy_2O_3. The P-B ratio of Dy_2O_3/Dy shows high value of 1.26 and Dy_2O_3 can fill up the loose cavities of MgO to form a highly protective surface film, which can effectively separate the alloy substrate from the attacking air.

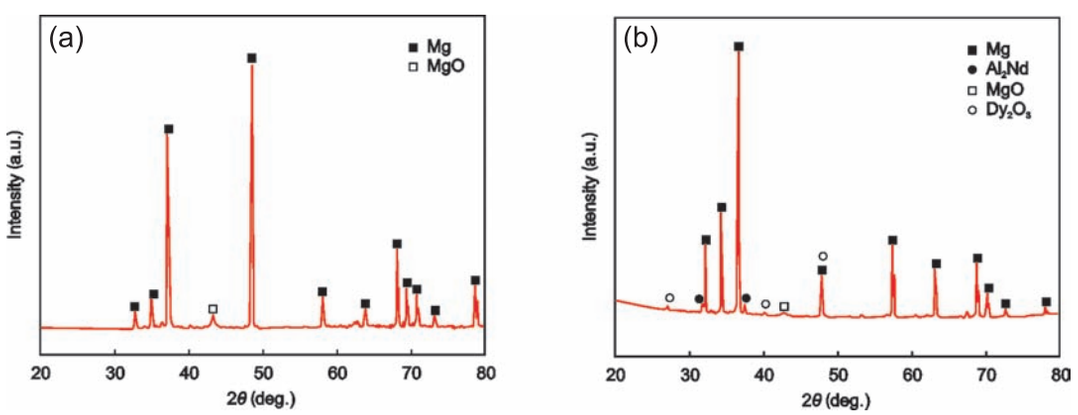

Fig. 6: XRD patterns for surface film of samples formed at 773 K holding 6 h: (a) AZ91D; (b) AZ91D-3Nd-2Dy

2.3.2 Cross-section characteristics of oxide film

Figure 7 shows the cross-section characteristics of the oxide film for both alloys which were formed at 773 K and held for 6 h. In Fig. 7(a), there are cracks and holes formed in the oxide film of AZ91D alloy, leading to the uneven and incomplete oxide film structure. In contrast, the oxide film of the AZ91D-3Nd-2Dy alloy is even, dense and well-bonded to the substrate [Fig. 7(b)]. It is obvious that the oxide film structure of the AZ91D-3Nd-2Dy alloy is more conducive to isolating the substrate from the air and thus improving the ignition-point.

2.3.3 Substrate characteristics of alloys

Figures 8 and 9 show the EDS mapping results of the cross-section image for the AZ91D and AZ91D-3Nd-2Dy alloys. In Figs. 8(a)–8(c), there are a large number of cracks in the AZ91D

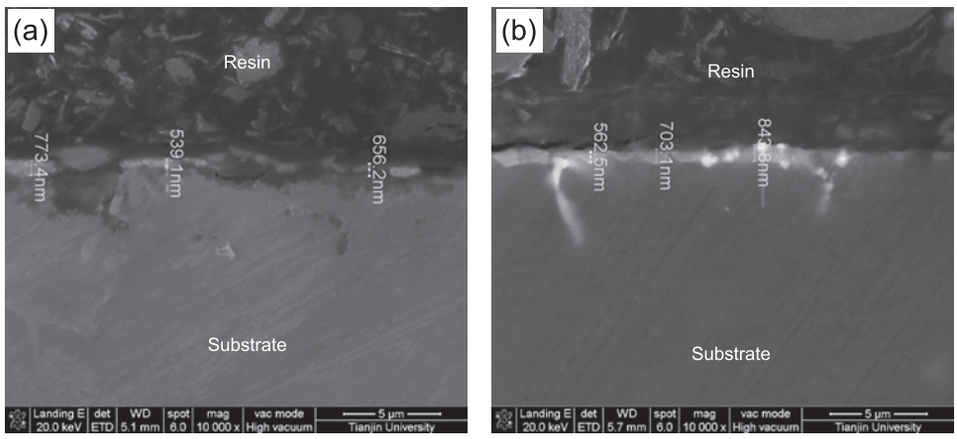

Fig. 7: Cross-section characteristics of oxide film formed at 773 K holding 6 h: (a) AZ91D; (b) AZ91D-3Nd-2Dy

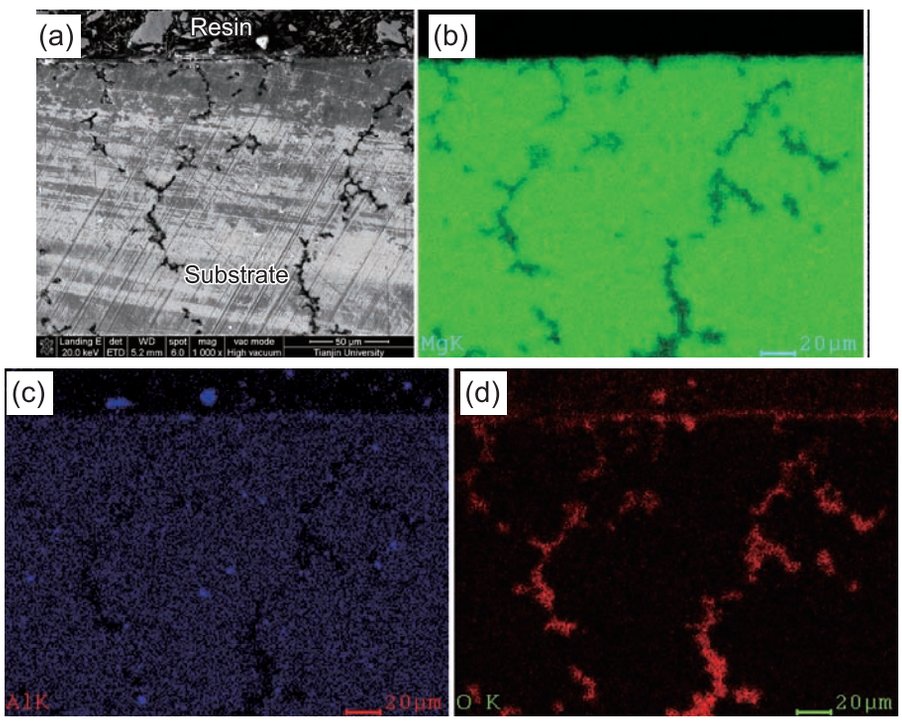

Fig. 8: EDS mapping results of Mg, Al and O for AZ91D alloy: (a) area of map scanning; (b) Mg; (c) Al; (d) O

alloy substrate near the alloy surface. The formation of these cracks is due to the melting of β-$Mg_{17}Al_{12}$ phase at 773 K as described in 2.3.1. From Fig. 8(d), it is observed that oxygen appears along the cracks, indicating that these cracks act as the continuous diffusion path of oxygen. During the penetration process of oxygen, it will react with Mg to form MgO accompanying with a lot of heat release. When the released heats accumulate to a certain degree, the alloy will ignite. So, it can be concluded that the formation of continuous cracks is the key factor of the low ignition-point for the AZ91D alloy.

It should be noted that, for the AZ91D-3Nd-2Dy alloy, the substrate is very dense, there are no obvious cracks [Fig. 9(a)], and O element only exists in the sample surface [Fig. 9(d)]. The black dotted-areas in Mg substrate [Fig. 9(b)] correspond exactly to the rich regions of Al, Nd and Dy [Figs. 9(c), 9(e), 9(f)]. As described in section 2.2, the black dotted-areas in the Mg substrate should be the Al_2Nd and Al_2Dy phases. Combined with Fig. 4(b), it can be seen that the newly formed high melting-point phase Al_2Nd and Al_2Dy, mixed with minor β-$Mg_{17}Al_{12}$ phase, exist mostly in the grain boundaries. When the Al_2Nd or Al_2Dy phase with a high melting point replace for the large portion of the β-$Mg_{17}Al_{12}$ phase located in the grain boundaries, the discrete Al_2Nd or Al_2Dy particles will act as the obstacle for the O element to diffuse through the channels, stopping or slowing down the melting of β-$Mg_{17}Al_{12}$, thus preventing the chemical reaction of Mg and oxygen.

3 Conclusions

This work studies the effect of the combined Nd and Dy addition on the ignition-proof performance of AZ91D alloy and the ignition-proof mechanism of AZ91D-3Nd-2Dy alloy at high temperatures. The obtained results can be summarized as follows:

(1) The combined addition of Nd and Dy can improve the ignition-proof performance of AZ91D alloy. The AZ91D-3Nd-2Dy alloy exhibits the highest ignition point of 893 K, an

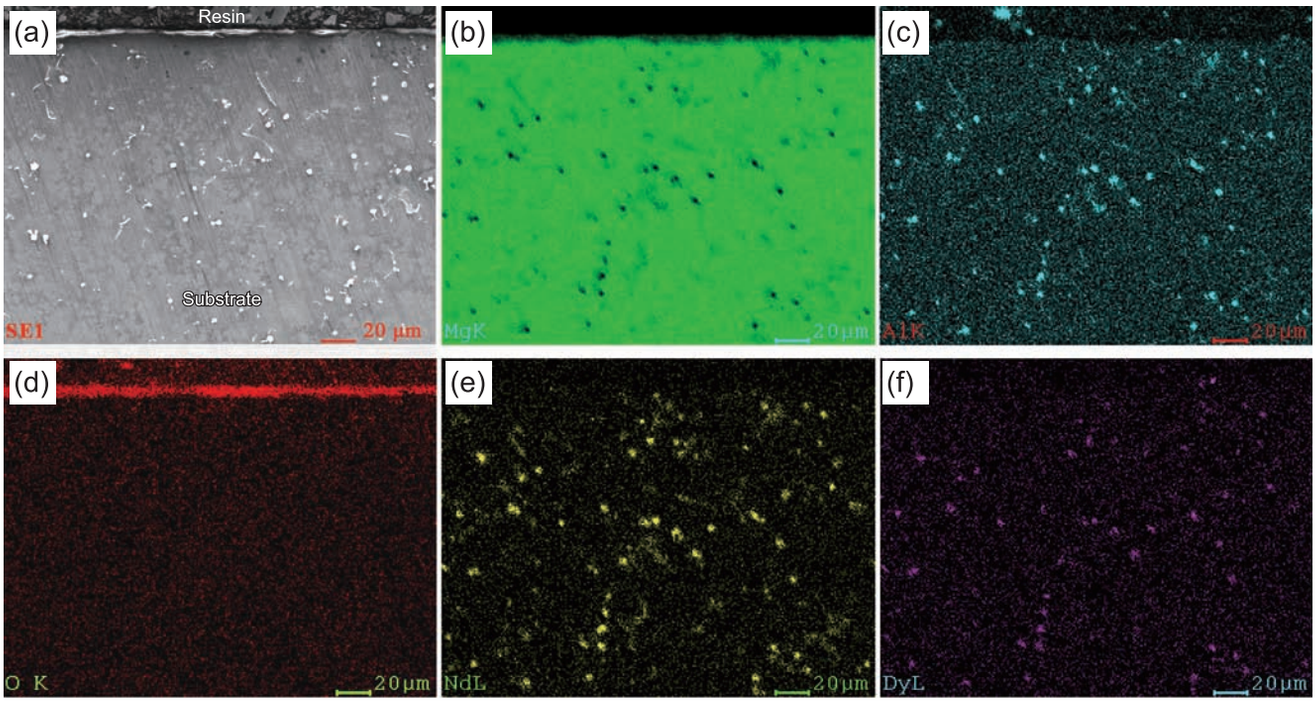

Fig. 9: EDS mapping results of Mg, Al, O, Nd and Dy for AZ91D-3Nd-2Dy alloy: (a) area of map scanning; (b) Mg; (c) Al; (d) O; (e) Nd; (f) Dy

increase of 69 K as compared to the AZ91D alloy.

(2) The ignition-proof mechanism of the AZ91D-3Nd-2Dy alloy at high temperatures mainly lies in three aspects:

Firstly, the surface oxide film of AZ91D-3Nd-2Dy formed at high temperature has a denser structure than that of AZ91D due to the filling of Dy_2O_3 into the pores of MgO film, helping the improvement in the oxidation resistance of the alloy.

Secondly, the addition of Nd and Dy can greatly reduce the formation of low melting-point phase β-$Mg_{17}Al_{12}$. Moreover, the distribution of β-$Mg_{17}Al_{12}$ changes from the continuous network along the grain boundaries in the AZ91D alloy to dispersed distribution in the AZ91D-3Nd-2Dy alloy, leading to the decrease in the oxygen diffusion channels.

Thirdly, for the AZ91D-3Nd-2Dy alloy, the newly formed high melting-point phases, Al_2Nd and Al_2Dy, mixed with minor β-$Mg_{17}Al_{12}$ phase, existing mostly at the grain boundaries, block the oxygen diffusion channels and prevent the chemical reaction of Mg and oxygen.

References

[1] Gwynne B A. Magnesium alloys in aerospace applications-flammability testing. TMS 2010 139th Annual Meeting & Exhibition. Washington, USA, 2010.
[2] Jeon J, Lee S, Kim B, et al. Effect of Sb and Sr addition on corrosion properties of Mg-5Al-2Si alloy. J. Korean Inst. Met. Mater, 2008, 46 (5): 304–309.
[3] Zhou Na, Zhang Zhenyan, Dong Jie, et al. Selective oxidation behavior of an ignition-proof Mg-Y-Ca-Ce alloy. J. Rare Earths, 2013, 31 (10): 1003–1008.
[4] Shih Tengshih, Liu Jyunbo, Wei Paisheng. Oxide films on magnesium and magnesium alloys. Mater. Chem. Phys, 2007, 104 (2–3): 497–504.
[5] Zeng Xiaoqin, Wang Qudong, Lü Yizhen, et al. Study on ignition proof magnesium alloy with beryllium and rare earth additions. Scr. Mater, 2000, 43 (5): 403–409.
[6] Fan J F, Yang Ch L, Han G, et al. Oxidation behavior of ignition-proof magnesium alloys with rare earth addition. J. Alloy. Compd, 2011, 509 (5): 2137–2142.
[7] Kim Y M, Yim C D, Kim H S, et al. Key factor influencing the ignition resistance of magnesium alloys at elevated temperatures. Scripta Mater., 2011, 65 (11): 958–961.
[8] Ha S H, Lee J K, Jo H H, et al. Behavior of CaO and Calcium in pure Magnesium. Rare Met., 2006, 25 (Z2): 150–154.
[9] Lin Pengyu, Zhou Hong, Li Wei, et al. Interactive effect of cerium and aluminum on the ignition point and the oxidation resistance of magnesium alloy. Corros Sci., 2008, 50 (9): 2669–2675.
[10] Zhang Guoying, Luo Zhicheng, Zhang Hui, et al. Igniton-proof mechanism of magnesium ally added with rare earth La from first-principle study. J. Rare Earths, 2012, 30 (6): 573–578.
[11] Fan Jianfeng, Chen Zhiyuan, Yang Weidong, et al. Effect of yttrium, calcium and zirconium on ignition-proof principle and mechanical properties of magnesium alloys. J. Rare Earths, 2012, 30 (1): 74–78.
[12] Zhao Hongjin, Zhang Yinghui, Kang Yonglin. Effect of cerium on ignition point of AZ91D magnesium ally. China Foundry, 2008, 5 (1): 32–35.
[13] Wang Xuemin, Zeng Xiaoqin, Wu Guosong, et al. The effect of alloy elements on the oxidation of Magnesium alloys. Materials Review, 2006, 20 (11): 69–72.
[14] Wang Jun, Wang Limin, An Jian, et al. Microstructure and Elevated Temperature Properties of Die-cast AZ91-xNd Magnesium Alloys. J. Mater. Eng. Perform, 2008, 17 (5): 725–729.
[15] Jin Liling, Y B Kang, Chartrand P, et al. Thermodynamic evaluation and optimization of Al-Gd, Al-Tb, Al-Dy, Al-Ho and Al-Er systems using a Modified Auasichemical Model for the liquid. Calphad, 2010, 34 (4): 456–466.
[16] Pilling N B, Bedworth R E. The oxidation of metals at high temperatures. J. Inst. Met., 1923, 29: 529–582.